the much stronger superconducting coherence peak suppressions (*8*, *10*, *22*, *23*) in Bi-2212. The analysis of correlations between the dopant defects and quasi-particle interference patterns $C[O(\vec{r}):LDOS(\vec{r},E)]$ shown in Fig. 4A reveals directly that they are strongly correlated over a wide energy range. The negative sign of these correlations means that minima of LDOS modulations preferentially occur at the dopant defects. This is true at all energies, even though the actual quasi-particle interference patterns are quite different (*8*). This can be seen directly in images of $LDOS(\vec{r},E)$ at $E = -14$ meV, -24 meV, and -34 meV (Fig. 4, B to D, respectively), with dopant defect locations shown as red dots. In all cases we see that the dopant defects have a very high probability of being found at the minima in the LDOS, even though the patterns are quite different between energies. This implies a fixing of the spatial phase of the LDOS modulations at scattering sites, an effect first seen in cuprates at oxygen vacancy defects in $YBa_2Cu_3O_{6-\delta}$ (*5*). Perhaps more important, Fig. 4D shows that suppression of superconducting coherence peaks is found primarily near the dopant defect clusters, and the bright regions with the sharp coherence peaks—usually associated with strong superconductivity—occur between them. The correspondence between dopant defect locations and LDOS minima for a variety of LDOS patterns occurring at different energies (Fig. 4) provides clear and direct evidence that these dopant defects generate the LDOS modulations and also suppress superconducting coherence peaks in Bi-2212.

Our simultaneous imaging of apparent dopant-induced impurity states and superconducting electronic structure points to solutions for several outstanding problems. The results provide direct evidence for the concept of an atomic-scale source for the nanoscale electronic disorder in cuprates (*11*, *24*–*26*). Strong correlations between dopant defect distributions and both gap map and coherence peak amplitude show that the dopant defects are responsible for most (but perhaps not all) of the superconducting electronic disorder in Bi-2212. Further, scattering leading to quasi-particle interference can now be ascribed almost completely to whichever atomic-scale perturbation produces the dopant defects. Finally, the topographic disorder and related superconducting electronic disorder are due empirically to spectral weight shifts from low to high energy near each dopant defect. These data indicate that high-energy spectral weight redistributions, strong coherence peak suppressions, and very weak scattering of low-energy quasi-particles are dominant elements in the atomic-scale mechanism of superconducting electronic disorder in $Bi_2Sr_2CaCu_2O_{8+\delta}$. Similar phenomena are likely to be common in all nonstoichiometric oxygen-doped high-T_c cuprates.

References and Notes

1. S. Maekawa *et al.*, *Physics of Transition Metal Oxides* (Springer-Verlag, Berlin, 2004).
2. R. J. Cava, *Nature* **394**, 126 (1998).
3. J. P. Attfield, A. L. Kharlanov, J. A. McAllister, *Nature* **394**, 157 (1998).
4. H. Eisaki *et al.*, *Phys. Rev. B* **69**, 064512 (2004).
5. H. L. Edwards *et al.*, *Phys. Rev. Lett.* **75**, 1387 (1995).
6. Y. Kohsaka *et al.*, *Phys. Rev. Lett.* **93**, 097004 (2004).
7. T. Hanaguri *et al.*, *Nature* **430**, 1001 (2004).
8. K. McElroy *et al.*, *Nature* **422**, 520 (2003).
9. G. Kinoda *et al.*, *Phys. Rev. B* **67**, 224509 (2003).
10. K. M. Lang *et al.*, *Nature* **415**, 412 (2002).
11. S. H. Pan *et al.*, *Nature* **413**, 282 (2001).
12. D. Grebille *et al.*, *Acta Crystallogr.* **B52**, 628 (1996).
13. W. Que, M. B. Walker, *Phys. Rev. B* **46**, 14772 (1992).
14. N. Miyakawa *et al.*, *Phys. Rev. Lett.* **80**, 157 (1998).
15. Q.-H. Wang, D.-H. Lee, *Phys. Rev. B* **67**, 020511 (2003).
16. L. Capriotti, D. J. Scalapino, R. D. Sedgewick, *Phys. Rev. B* **68**, 014508 (2003).
17. L. Zhu, W. A. Atkinson, P. J. Hirschfeld, *Phys. Rev. B* **69**, 060503 (2004).
18. U. Chatterjee *et al.*, available at http://arXiv.org/abs/cond-mat/0505296.
19. K. McElroy *et al.*, available at http://arXiv.org/abs/cond-mat/0505333.
20. T. Cren *et al.*, *Europhys. Lett.* **54**, 84 (2001).
21. A. Matsuda *et al.*, *Physica C* **388**, 207 (2003).
22. C. Howald, P. Fournier, A. Kapitulnik, *Phys. Rev. B* **64**, 100504 (2001).
23. K. McElroy *et al.*, *Phys. Rev. Lett.* **94**, 197005 (2005).
24. Z. Wang *et al.*, *Phys. Rev. B* **65**, 064509 (2002).
25. Q.-H. Wang, J. H. Han, D.-H. Lee, *Phys. Rev. B* **65**, 054501 (2002).
26. I. Martin, A. V. Balatsky, *Physica C* **357–360**, 46 (2001).
27. D. J. Scalapino, T. S. Nunner, P. J. Hirschfeld, in *Proceedings of the 7th International Conference on Spectroscopies in Novel Superconductors* (*Sitges, Spain*), in press (available at http://arXiv.org/abs/cond-mat/0409204).
28. J.-X. Zhu *et al.*, *Phys. Rev. Lett.* **91**, 057004 (2003).
29. E. Kaneshita, I. Martin, A. R. Bishop, *Phys. Soc. Jpn. Lett.* **73**, 3223 (2004).
30. J. Bobroff *et al.*, *Phys. Rev. Lett.* **89**, 157002 (2002).
31. J. W. Loram, J. L. Tallon, W. Y. Liang, *Phys. Rev. B* **69**, 060502 (2004).
32. T. Nunner *et al.*, available at http://arXiv.org/abs/cond-mat/0504693.

33. We thank W. Atkinson, A. V. Balatsky, A. Bishop, J. C. Campuzano, R. J. Cava, P. Hirschfeld, J. E. Hoffman, V. Madhavan, R. Markiewicz, T. M. Rice, G. Sawatzky, D. J. Scalapino, Z.-X. Shen, Z. Wang, and A. Yazdani for helpful conversations and communications. Supported by the Office of Naval Research, NSF, and Cornell University.

4 April 2005; accepted 30 June 2005
10.1126/science.1113095

FD, a bZIP Protein Mediating Signals from the Floral Pathway Integrator FT at the Shoot Apex

Mitsutomo Abe,[1]* Yasushi Kobayashi,[1,2]*† Sumiko Yamamoto,[1,2]* Yasufumi Daimon,[1] Ayako Yamaguchi,[1] Yoko Ikeda,[1] Harutaka Ichinoki,[1] Michitaka Notaguchi,[1] Koji Goto,[2,3] Takashi Araki[1,2,4]‡

FLOWERING LOCUS T (*FT*) is a conserved promoter of flowering that acts downstream of various regulatory pathways, including one that mediates photoperiodic induction through *CONSTANS* (*CO*), and is expressed in the vasculature of cotyledons and leaves. A bZIP transcription factor, FD, preferentially expressed in the shoot apex is required for FT to promote flowering. FD and FT are interdependent partners through protein interaction and act at the shoot apex to promote floral transition and to initiate floral development through transcriptional activation of a floral meristem identity gene, *APETALA1* (*AP1*). *FT* may represent a long-distance signal in flowering.

Flowering in *Arabidopsis* is regulated by several pathways that converge on the transcriptional regulation of the floral pathway integrators *FT*, *SUPPRESSOR OF OVEREXPRESSION OF CO 1* (*SOC1*), and *LEAFY* (*LFY*) (*1*). *FT* is a direct target of CO, a key transcriptional regulator of the photoperiod pathway, and the role of *FT* as a potent promoter of flowering in response to photoperiods is conserved in *Arabidopsis* and rice (*2*–*6*). *FT* is expressed in the phloem tissues of cotyledons and leaves (*7*, *8*) and encodes a 20-kD protein with homology to phosphatidylethanolamine binding protein or Raf kinase inhibitor protein (*2*, *3*). However, the biochemical function of FT and downstream events leading to floral transition and floral morphogenesis at the shoot apex remain unknown.

bZIP protein FD is required for FT function. To understand how signals are mediated from *FT* to finally cause floral transition and floral morphogenesis, we searched for genes required for *FT* to promote flowering. Ectopic

[1]Department of Botany, Graduate School of Science, Kyoto University, Sakyo-ku, Kyoto 606-8502, Japan. [2]CREST, Japan Science and Technology Agency, Kawaguchi 332-0012, Japan. [3]Research Institute for Biological Sciences Okayama, Okayama 716-1241, Japan. [4]Adjunct Division of Applied Genetics, National Institute of Genetics, Mishima 411-8540, Japan.

*These authors contributed equally to this work.
†Present address: Department of Molecular Biology, Max Planck Institute for Developmental Biology, D-72076 Tübingen, Germany.
‡To whom correspondence should be addressed. E-mail: taraqui@cosmos.bot.kyoto-u.ac.jp

Table 1. Flowering times of transgenic and mutant plants.

Genotype*	No. of rosette leaves†	No. of cauline leaves†	*N*
	Experiment 1, LDs		
Wild type (Col)	14.2 ± 2.2 (11–18)	3.0 ± 0.7 (2–4)	25
fd-1	23.1 ± 3.1 (19–29)	6.6 ± 1.2 (4–8)	14
35S::FT (YK#1-5C)	2.8 ± 0.4 (2–3)	1.0 ± 0.4 (0–2)	25
35S::FT (YK#1-5C); *fd-1*	18.4 ± 2.7 (14–24)	5.4 ± 1.2 (4–8)	20
soc1-101D‡	1.9 ± 0.3 (1–2)§	2.1 ± 0.3 (2–3)	15
soc1-101D; fd-1‡	2.0 ± 0 (2)	1.9 ± 0.3 (1–2)	21
Wild type (L*er*)	7.2 ± 1.1 (6–9)	2.4 ± 0.8 (1–4)	22
fd-1	12.3 ± 0.7 (11–15)	4.1 ± 0.7 (3–5)	43
35S::FT (YK#1-5L)	2.0 ± 0 (2)	1.2 ± 0.4 (1–2)	40
35S::FT (YK#1-5L); *fd-1*	4.0 ± 0 (4)	2.4 ± 0.8 (1–4)	24
	Experiment 2, SDs		
Wild type (Col),	45.3 ± 5.1 (38–54)	10.4 ± 2.0 (7–15)	17
fd-1	51.0 ± 5.8 (43–61)	9.8 ± 1.7 (7–13)	15
35S::FT (YK#1-5C)	2.3 ± 0.5 (2–3)	1.0 ± 0.5 (0–2)	25
35S::FT (YK#1-5C); *fd-1*	18.2 ± 4.3 (11–26)	4.4 ± 1.1 (3–7)	19
	Experiment 3, LDs		
Wild type (L*er*)	5.3 ± 0.5 (5–6)	1.7 ± 0.5 (1–2)	14
ft-3‡	11.2 ± 0.8 (10–12)	2.8 ± 0.4 (2–3)	10
FD::FT (YD#2-1); *ft-3*	3.5 ± 0.5 (3–4)	0.5 ± 0.5 (0–1)	14
PDF1::FT (MA#4-12); *ft-3*	2.1 ± 0.4 (2–3)	1.0 ± 0.5 (0–2)	35
SULTR2;1::FT (YD#1-1); *ft-3*	3.0 ± 0 (3)	0.7 ± 0.5 (0–1)	15
IAA14::FT (YD#4-3); *ft-3*‡	10.7 ± 0.8 (9–12)	2.4 ± 0.5 (2–3)	20
	Experiment 4, LDs		
Wild type (Col)	10.0 ± 0.7 (9–12)	2.4 ± 0.6 (1–3)	21
fd-1‡	21.1 ± 2.0 (18–24)	5.5 ± 0.5 (5–6)	22
FD::FD (MN#7-1); *fd-1*	8.4 ± 0.5 (8–9)	2.9 ± 0.5 (2–4)	21
SULTR2;1::FD (MN#4-2); *fd-1*‡	20.7 ± 1.6 (18–24)	5.0 ± 0.7 (4–6)	23
	Experiment 5, LDs		
Wild type (L*er*)	5.3 ± 0.5 (5–6)	1.8 ± 0.4 (1–2)	15
ft-3	13.7 ± 0.7 (12–15)	3.3 ± 0.7 (2–5)	15
ft-3; fd-1	17.8 ± 0.8 (16–19)	5.3 ± 0.4 (5–6)	16
FD::FT (YD#2-1); *ft-3*	2.9 ± 0.6 (2–4)	0.8 ± 0.4 (0–1)	15
FD::FT (YD#2-1); *ft-3; fd-1*	5.9 ± 0.6 (5–7)	1.8 ± 0.6 (1–3)	15
PDF1::FT (MA#4-12); *ft-3*	2.0 ± 0 (2)	1.3 ± 0.5 (1–2)	18
PDF1::FT (MA#4-12); *ft-3*; *fd-1*	6.4 ± 0.6 (5–7)	2.5 ± 0.5 (2–3)	20
SULTR2;1::FT (YD#1-1); *ft-3*	2.7 ± 0.5 (2–3)	1.2 ± 0.4 (1–2)	13
SULTR2;1::FT (YD#1-1); *ft-3; fd-1*	4.1 ± 0.3 (4–5)	2.0 ± 0 (2)	13
	Experiment 6, LDs		
Wild type (L*er*), –Dex	6.8 ± 0.9 (5–8)	3.0 ± 0.6 (2–4)	22
Wild type (L*er*), +Dex‖	6.4 ± 0.9 (5–8)	2.9 ± 0.7 (2–4)	24
ft-3, −Dex	14.1 ± 2.5 (11–19)	4.9 ± 1.0 (4–7)	12
ft-3, +Dex‖	12.7 ± 1.8 (10–15)	4.2 ± 0.6 (3–5)	11
35S::FT:GR (YD#9-a); *ft-3*, −Dex	8.8 ± 1.7 (6–12)	3.7 ± 0.6 (3–5)	24
35S::FT:GR (YD#9-a); *ft-3*, +Dex	3.3 ± 0.7 (2–4)	2.1 ± 0.4 (1–3)	24

*Genetic background: Col, Columbia; L*er*, Landsberg *er*. Plants in each experiment were grown under LDs or SDs as indicated. +Dex indicates Dex treatment (*14*). †Indicators of flowering time (*10*) and shown as average ± SD (range). Statistical tests were done on the number of rosette leaves. ‡No statistically significant difference among indicated genotypes in each experiment (Student's *t* test, $P > 0.1$). No symbol means that there was a statistically significant difference ($P < 0.001$) among the genotypes or conditions compared in each experiment. §Includes two plants with elongated internodes. ‖Indicates no statistically significant difference from the above condition ($P > 0.06$).

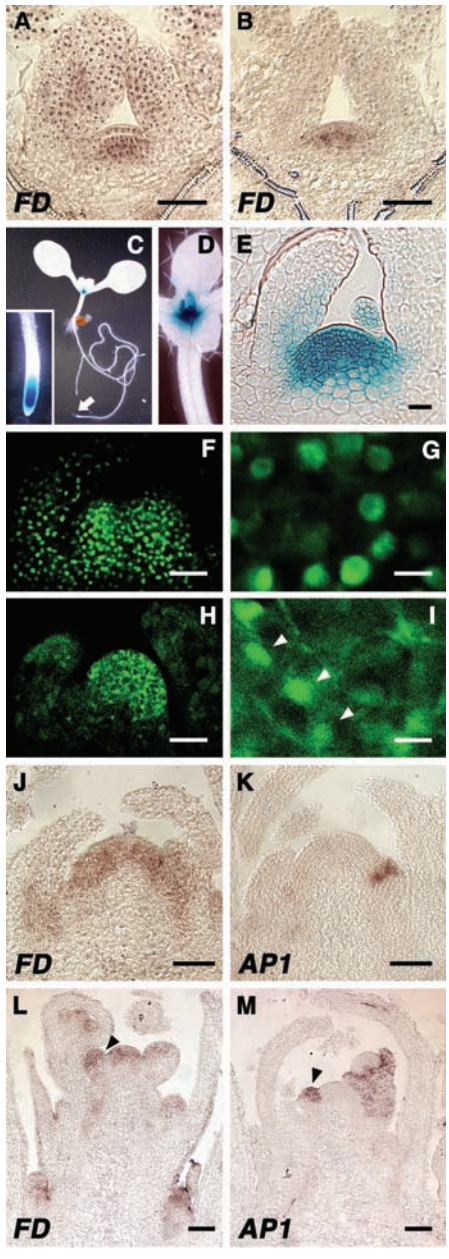

Fig. 1. Expression of *FD* and subcellular distribution of EGFP:FD and FT:EGFP. (**A** and **B**) Expression of *FD* in shoot apex of wild-type seedlings grown under LDs (16 hours light) for 6 (A) and 7 (B) days. (**C** to **E**) GUS staining of *gFD::GUS* seedlings grown under LDs for 6 (C and D) and 7 (E) days. (C) A whole seedling. The arrow indicates a root tip, which is enlarged in the inset. (D) Shoot apical region. (E) Longitudinal section of shoot apex. (**F** to **I**) Distribution of functional EGFP:FD fusion protein (F and G) and functional FT:EGFP fusion protein (H and I) expressed in shoot apex by *FD* promoter. (G) and (I) are enlargements showing subcellular distribution. Arrowheads in (I) indicate nuclei. (**J** to **M**) Expression of *FD* (J and L) and *AP1* (K and M) in shoot apex of wild-type plants at floral transition on day 10 (J and K) and early inflorescence stage on day 15 (L and M) under LDs. Arrowheads in (L) and (M) indicate floral meristems at stage 1. Scale bars: 50 μm in (F), (H), (L), and (M); 20 μm in (A), (B), (E), (J), and (K); and 10 μm in (G) and (I).

overexpression of *FT* by the 35*S* RNA promoter of cauliflower mosaic virus (*35S::FT*) causes a precocious-flowering phenotype (*2*, *3*). We screened for suppressors of *35S::FT*, because a similar approach with *35S::CO* was successful in elucidating the downstream targets of CO, *FT* and *SOC1* (*4*, *9*). In addition to screening mutagenized populations of *35S::FT*, we examined known late-flowering mutants (*10*) for their effect on the *35S::FT* phenotype. Through the latter approach, we found that *fd-1* is a strong suppressor of *35S::FT* (Table 1). In contrast to a strong effect on *35S::FT*, *fd-1* had only a weak effect on a similar precocious-flowering phenotype of *soc1-101D*, an activation tagged allele of *SOC1* (*11*) (Table 1), or *35S::LFY* (*12*). These observations suggest that the *FD* activity is required specifically for the promotion of flowering by *FT*.

The *FD* gene was identified with *AtbZIP14* (At4g35900) (*13*) by a map-based approach (figs. S1 and S2 and table S1). In seedlings, *FD* expression was observed mainly in the shoot apex (Fig. 1, A to E and J), did not show distinct circadian oscillation, and was not affected by photoperiods and *CO* activity (fig. S3). Under both short days (SDs) and long days (LDs), *FD* mRNA levels increased with time after germination (fig. S3). To examine the subcellular distribution of FD protein, we made a construct

to express enhanced green fluorescent protein–FD (EGFP:FD) fusion protein by the *FD* promoter (*FD::EGFP:FD*) (*14*). That the fusion protein is functional was confirmed by the rescue of *fd-1* (table S2). EGFP:FD was localized in the nucleus in cells of the shoot apex (Fig. 1, F and G). Similarly, nuclear localization of functional enhanced yellow fluorescent protein–FD (EYFP:FD) fusion protein (table S2) was observed in cells of the shoot apex and other tissues in *35S::EYFP:FD* seedlings with various genetic backgrounds (fig. S4) (*14*), suggesting a constitutive nuclear localization.

To gain clues to the molecular basis of the requirement of *FD* for *FT* function, we investigated protein interactions. FT interacted with FD in yeast cells (Fig. 2A) and in vitro (Fig. 2C). In contrast, FD showed very weak interaction in yeast cells with TERMINAL FLOWER 1 (TFL1), the FT-related protein with an antagonistic role in the regulation of flowering (*2*, *3*) (Fig. 2A and fig. S5). Because the subcellular distribution of the FT protein remains unknown, we examined the distribution of functional FT:EGFP fusion protein (table S2) expressed in the shoot apex of *Arabidopsis* by the *FD* promoter or in leaf epidermal cells of *Nicotiana benthamiana* by the 35*S* promoter (*14*). In both cases, FT:EGFP was observed in the nucleus and cytoplasm (Fig. 1, H and I, and fig. S4). That FT is able to function in the nucleus was supported by observations that FT protein fused to a glucocorticoid receptor (GR) expressed by the 35*S* promoter (*35S::FT:GR*) (*14*) promoted flowering on dexamethasone (Dex) treatment (Table 1). These findings suggest that FD and FT proteins coexist in the nucleus. We further analyzed the interaction of FT and FD proteins in plant cells using bimolecular fluorescent complementation (BiFC) (*15*). In tobacco leaf epidermal cells coexpressing the N-terminal half of EYFP fused to FD (YN-FD) and the C-terminal half of EYFP fused to FT (YC-FT) (*14*), YFP fluorescence was observed in the nucleus (Fig. 2D). These findings show that protein interaction is the basis of the dependence of FT on FD.

Floral meristem identity genes are regulatory targets of FT and FD. We next tried to identify the regulatory targets of FT and FD in the shoot apex that cause floral transition and morphogenesis. We obtained clues from analysis of *ft; lfy* and *fd; lfy* double mutants. A previous work showed that *ft; lfy* greatly reduced mRNA levels of *AP1* and caused severe defects in floral meristem specification (*16*). These observations led to the suggestion that *FT* and *LFY* play redundant roles in up-regulation of *AP1* and floral fate specification (*1*, *16*). In agreement with a previous report, *ft; lfy* greatly reduced the amount and region of *AP1* expression in the shoot apex and caused severe defects in floral development (Fig. 3, A to D, and fig. S6). *fd; lfy* plants had an inflorescence phenotype indistinguishable from that of *ft; lfy* and displayed a severely reduced amount and spatial extent of *AP1* expression (Fig. 3, A to D, and fig. S6). These observations suggest that *FT* and *FD* together are involved in the regulation of *AP1* redundantly with *LFY*.

Consistent with a role of FD in the regulation of *AP1*, ectopic expression of *AP1* was observed in *35S::FD* seedlings (Fig. 3E). Ectopic induction of *AP1* expression by FD was abolished by *ft* mutation (Fig. 3F) or under SDs, which reduce *FT* expression (*2*, *3*, *17*, *18*) (Fig. 3G). Upon a shift from SDs to LDs, which induces *FT* expression (*8*, *18*), *AP1* expression was induced (Fig. 3H). In young seedlings, *FT* is expressed mainly in the vasculature of cotyledons, and little is detected in mesophyll cells (*7*, *8*). In *35S::FD* seedlings, *AP1* expression was detected in the vascular-rich fraction but not in the mesophyll-rich fraction from cotyledons (Fig. 3I). These observations suggest that activation of *AP1* expression by FD requires the *FT* function. Finally, in the shoot apex around the stage of floral transition and in the young inflorescence apex, the region of *AP1* expression was within the expression domain of *FD* (Fig. 1, J to M). Thus, *AP1* seems to be a regulatory target of FD, which requires the FT activity through protein interaction. In support of this conclusion, several potential bZIP protein binding motifs were found in a 1.7-kb *AP1* promoter (*19*) (fig. S7).

Because *AP1* expression was observed only in a subset of the expression domain of *FD*, there should be factors that restrict *AP1* expression to nascent lateral meristems. *TFL1*, which has a role antagonistic to *FT* (*2*, *3*), is likely to be responsible for suppressing *AP1* expression in the shoot apical meristem proper (*20*, *21*). That the loss of *AP1* alone does not affect the precocious-flowering phenotype of *35S::FT* (*3*) suggests that other regulatory targets of FD contribute to the promotion of floral transition. *FRUITFULL* (*FUL*) and *CAULIFLOWER* (*CAL*), which act redundantly with *AP1* to promote flowering (*22*), are candidates for such targets (Fig. 3, C and E to J, and fig. S8).

How FT regulates FD activity is another important question. Constitutive nuclear localization of FD and the presence of FT in the nucleus suggest the regulation of FD activity in the nucleus. Whether FD and FT form a stable transcriptional complex or interact only transiently remains to be investigated. FD protein has a potential phosphorylation site for Ca^{2+}-dependent protein kinases (CDPKs) at the C terminus (Fig. 2B and fig. S2). Deletion or mutation of this

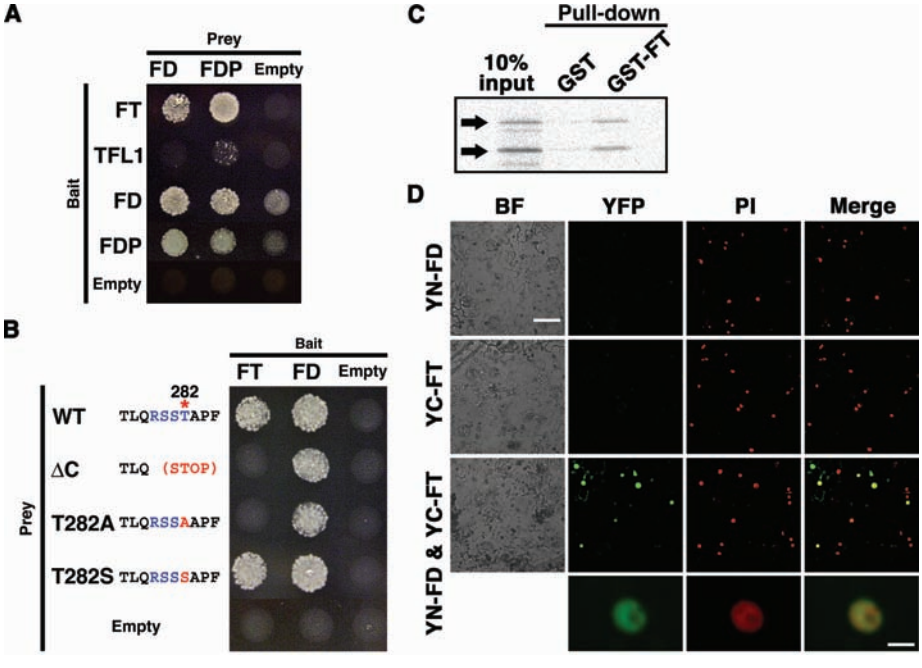

Fig. 2. Protein interaction. (**A**) Yeast two-hybrid assay of interaction among FD, FDP, FT, and TFL1. FDP, FD PARALOG (AtbZIP27). (**B**) Yeast two-hybrid assay of interaction between FT and C-terminal mutants of FD. C-terminal sequences of wild-type (WT) FD and mutant (ΔC, T282A, T282S) FD proteins including a possible CDPK site (blue). The asterisk on the WT sequence indicates a threonine (T) residue expected to be phosphorylated. T282A (substitution with an alanine), but not T282S (substitution with a serine), abolishes the CDPK site. None of the mutants affected interaction with wild-type FD. (**C**) In vitro pull-down assay of interaction between FT and FD (*14*). "10% input" indicates 10% of ^{35}S-labeled FD subjected to pull-down by GST or GST-FT. Arrows indicate labeled FD. (**D**) BiFC analysis of interaction between FT and FD in *N. benthamiana* leaf epidermis (*14*). BF, blight field image; YFP, YFP fluorescence; PI, propidium iodide fluorescence (nuclei); Merge, merge of YFP and PI; YN-FD, expression of YN-FD alone; YC-FT, expression of YC-FT alone; YN-FD & YC-FT, coexpression of YN-FD and YC-FT. At the bottom are higher magnification images of a nucleus of a cell coexpressing YN-FD and YC-FT. Not all nuclei were stained with PI. Scale bars: 100 μm (upper three rows) and 10 μm (bottom row).

site abolished interaction with FT (Fig. 2B), ectopic induction of *AP1* expression (Fig. 3J), and the ability to complement *fd-1* (fig. S9), although nuclear localization was not affected (fig. S4). These findings suggest the importance of phosphorylation of FD in the interaction with FT and in its functional regulation.

Mutual dependence and site of action of FT and FD. The mutual dependence of *FT* and *FD*, as shown above, is further supported by the observation that flowering of *35S::EYFP:FD* plants was delayed under SDs, which reduce *FT* expression (table S3). Furthermore, the enhanced phenotype in *35S::FT; 35S::FD* (tables S3 and S4) indicates that *FT* and *FD* are mutually limiting for the combined activity of *FT* and *FD*. These raise the question of the site(s) of action of FT and FD. In seedlings, *FT* is expressed in the vasculature of cotyledons, but not in the shoot apex (*7*) (fig. S10), whereas *FD* is expressed in the shoot apex but not in cotyledons and leaves (Fig. 1, A to E, and fig. S10). As expected, restoration of the *FT* function in the vasculature through expression by *SULTR2;1::FT* (*14*) could rescue the late-flowering phenotype of *ft* (Table 1 and table S5). Restoration of the *FT* function in the shoot apex of *ft*, either in the whole region by *FD::FT* or in the outermost cell layer (L1) by *PDF1::FT* (*14*), also rescued the late-flowering phenotype (Table 1 and table S5). These findings agree well with those of a previous report that the late-flowering phenotype of *co* is suppressed by similar constructs for *FT* misexpression (*23*). We further observed that *FD::FT*, *PDF1::FT*, and *SULTR2;1::FT* rescued delayed flowering, reduced *AP1* expression, and severe floral defect in *ft; lfy* (Fig. 3, B and C, and fig. S6). By contrast, restoration of *FT* in root vasculature by *IAA14::FT* (*14*) failed to rescue *ft* (Table 1). These observations indicate that ectopically expressed *FT* in the shoot apex can exert an effect on flowering. *FT* expressed in the shoot apex requires the *FD* function, because *fd-1* attenuated the rescued phenotype (Table 1 and table S5). In contrast, *FD* rescued the late-flowering phenotype of *fd* through expression in the whole shoot apex (by *FD::FD*), but not through ectopic expression in leaf vasculature (by *SULTR2;1::FD*), where *FT* is expressed (Table 1). Therefore, *FD* acts in the shoot apex and seems to be required in all cell layers. These findings, together with observations that protein interaction is the basis for interdependence between FT and FD, suggest that the shoot apex is the site of the *FT* and *FD* action.

FT and the long-distance signal in flowering. It has long been believed that a long-distance signal, named florigen (*24*), is generated in leaves upon exposure to inductive photoperiods, is transported to the shoot apex, and acts there to promote flowering (*25*). However, the nature of the signal has remained elusive (*25*). Our present work supports an emerging hypothesis (*7*, *8*, *23*) that the *FT* products represent a part of the long-distance signal(s) generated in cotyledons and leaves (mainly in the phloem tissues) and act at the shoot apex to promote floral transition and to initiate floral development (fig. S11).

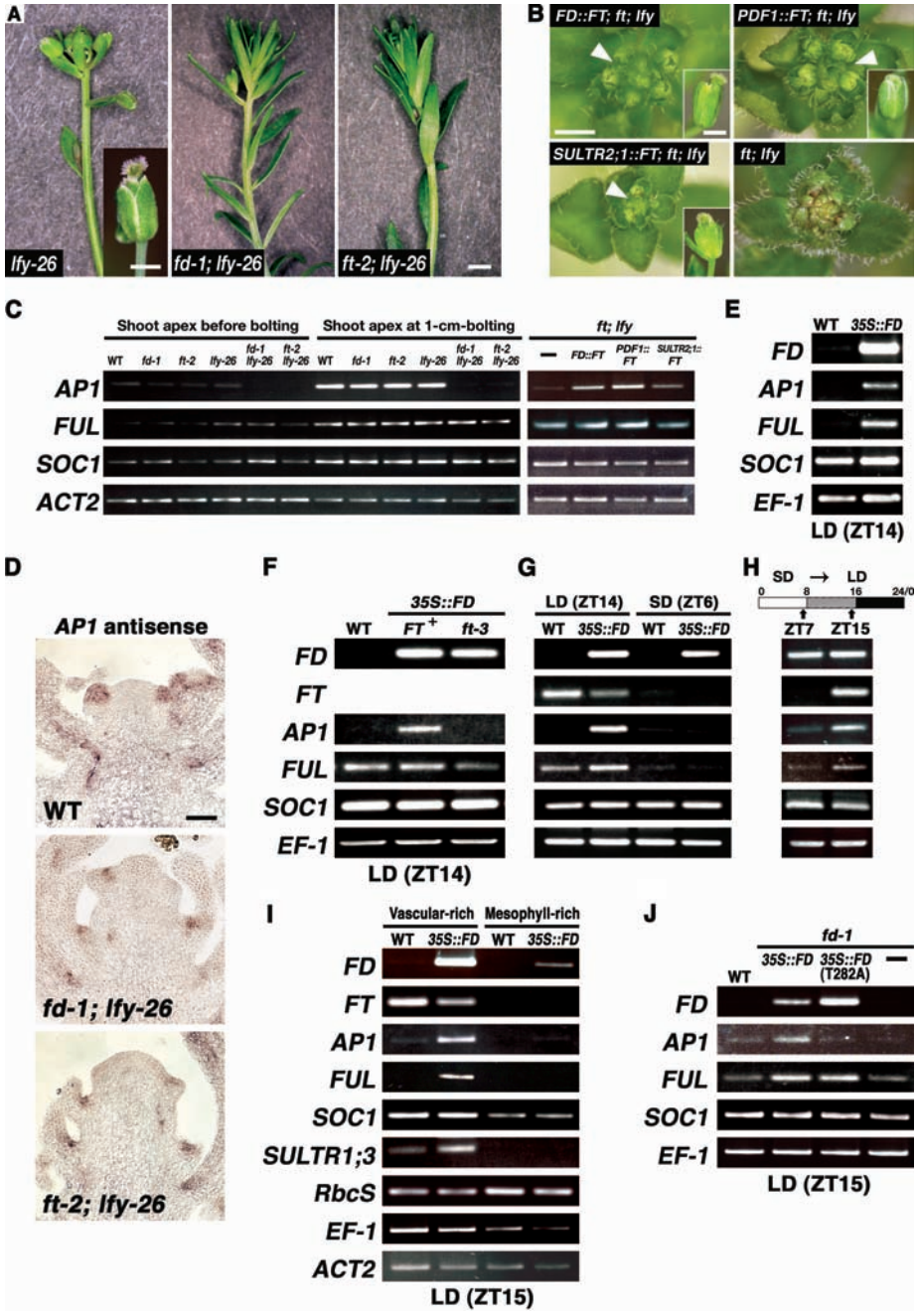

Fig. 3. *FT*-dependent activation of *AP1* by FD. (**A**) Floral defect in *lfy-26*, *fd-1; lfy-26*, and *ft-2; lfy-26*. Lateral structures on the primary inflorescence that would be single flowers in the wild-type plant. Inset shows a flower formed later in *lfy-26*. Scale bars: 2 mm and 1 mm (inset). (**B**) Rescue of floral defect in *ft-2; lfy-26* by tissue-specific expression of *FT*. Young primary inflorescences and flowers of *ft-2; lfy-26* with indicated *FT* constructs. Arrowheads indicate a terminal flower. Scale bars, 2 mm and 1 mm (inset). (**C**) *AP1* and *FUL* expression in shoot apex of various genotypes at two different stages. *SOC1* and *ACT2* were amplified for reference. (**D**) *AP1* expression in young inflorescence apex. Scale bar: 10 μm. (**E** to **J**) *AP1* and *FUL* expression in *35S::FD* and wild-type (WT) seedlings. *SOC1*, *EF-1*, and *ACT2* were amplified for reference. Whole seedlings (E to H and J) or cotyledons (I) were harvested for RNA extraction at the indicated Zeitgeber time (ZT) points. (E) Seven-day-old seedlings under LDs. (F) Seven-day-old *35S::FD* in FT^{+} and *ft-3* background and wild type under LDs. (G) Seven-day-old seedlings under LDs and SDs (8 hours light). (H) *35S::FD* seedlings grown for 6 days under SDs and subjected to day-length extension from 8 to 16 hours on day 7. (I) Vascular- and mesophyll-rich fractions from cotyledons of 10-day-old seedlings under LDs (*14*). *SULTR1;3* is a vascular marker and *RbcS* is preferentially expressed in mesophylls. (J) Seven-day-old seedlings of wild-type and *fd-1* with *35S::FD* or $35S::FD^{T282A}$ or without a transgene (−) under LDs.

References and Notes

1. G. G. Simpson, C. Dean, *Science* **296**, 285 (2002).
2. Y. Kobayashi, H. Kaya, K. Goto, M. Iwabuchi, T. Araki, *Science* **286**, 1960 (1999).
3. I. Kardailsky *et al.*, *Science* **286**, 1962 (1999).
4. A. Samach *et al.*, *Science* **288**, 1613 (2000).
5. S. Kojima *et al.*, *Plant Cell Physiol.* **43**, 1096 (2002).
6. R. Hayama, S. Yokoi, S. Tamaki, M. Yano, K. Shimamoto, *Nature* **422**, 719 (2003).
7. S. Takada, K. Goto, *Plant Cell* **15**, 2856 (2003).
8. A. Yamaguchi, Y. Kobayashi, K. Goto, M. Abe, T. Araki, *Plant Cell Physiol.* **46**, 1175 (2005).
9. H. Onouchi, M. I. Igeño, C. Périlleux, K. Graves, G. Coupland, *Plant Cell* **12**, 885 (2000).
10. M. Koornneef, C. J. Hanhart, J. H. van der Veen, *Mol. Gen. Genet.* **229**, 57 (1991).
11. H. Lee *et al.*, *Genes Dev.* **14**, 2366 (2000).
12. O. Nilsson, I. Lee, M. A. Blázquez, D. Weigel, *Genetics* **150**, 403 (1998).
13. M. Jakoby *et al.*, *Trends Plant Sci.* **7**, 106 (2002).
14. Materials and methods are available as supporting material on *Science* Online.
15. C. D. Hu, Y. Chinenov, T. K. Kerppola, *Mol. Cell* **9**, 789 (2002).
16. L. Ruiz-García *et al.*, *Plant Cell* **9**, 1921 (1997).
17. P. Suárez-López *et al.*, *Nature* **410**, 1116 (2001).
18. M. J. Yanovsky, S. A. Kay, *Nature* **419**, 308 (2002).
19. F. D. Hempel *et al.*, *Development* **124**, 3845 (1997).
20. O. J. Ratcliffe, D. J. Bradley, E. S. Coen, *Development* **126**, 1109 (1999).
21. S. J. Liljegren, C. Gustafson-Brown, A. Pinyopich, G. S. Ditta, M. F. Yanofsky, *Plant Cell* **11**, 1007 (1999).
22. C. Ferrándiz, Q. Gu, R. Martienssen, M. F. Yanofsky, *Development* **127**, 725 (2000).
23. H. An *et al.*, *Development* **131**, 3615 (2004).
24. M. K. Chailakhyan, *C. R. (Dokl.) Acad. Sci. URSS* **16**, 227 (1937).
25. J. A. D. Zeevaart, *Annu. Rev. Plant Physiol.* **27**, 321 (1976).
26. We thank P. Wigge and D. Weigel for the exchange of unpublished results; M. Koornneef, I. Lee, Y. Komeda, T. Takahashi, H. Takahashi, H. Fukaki, E. Lifschitz, G. Coupland and Plant Bioscience Limited, I. Hara-Nishimura, and the NSF-supported Arabidopsis Biological Resource Center for materials; M. Endo for technical advice; and Y. Tomita for technical assistance. Supported by grants from the Ministry of Education, Culture, Sports, Science and Technology of Japan (to T.A. and M.A.), the Core Research for Evolutional Science and Technology (CREST) program of the Japan Science and Technology Agency (to T.A.), and the Promotion of Basic Research Activities for Innovative Biosciences (PROBRAIN) program of the Bio-oriented Technology Research Advancement Institution, Japan (to M.A.).

Supporting Online Material
www.sciencemag.org/cgi/content/full/309/5737/1052/DC1
Materials and Methods
SOM Text
Tables S1 to S5
Figs. S1 to S11
References

10 June 2005; accepted 12 July 2005
10.1126/science.1115983

Integration of Spatial and Temporal Information During Floral Induction in *Arabidopsis*

Philip A. Wigge,[1,4]*†‡ Min Chul Kim,[1]* Katja E. Jaeger,[1]† Wolfgang Busch,[2] Markus Schmid,[3] Jan U. Lohmann,[2] Detlef Weigel[1,4]‡

Flowering of *Arabidopsis* is regulated by several environmental and endogenous signals. An important integrator of these inputs is the *FLOWERING LOCUS T* (*FT*) gene, which encodes a small, possibly mobile protein. A primary response to floral induction is the activation of *FT* RNA expression in leaves. Because flowers form at a distant site, the shoot apex, these data suggest that *FT* primarily controls the timing of flowering. Integration of temporal and spatial information is mediated in part by the bZIP transcription factor FD, which is already expressed at the shoot apex before floral induction. A complex of FT and FD proteins in turn can activate floral identity genes such as *APETALA1* (*AP1*).

One of the major flowering pathways in *Arabidopsis*, the photoperiod pathway, positively regulates activity of the nuclear protein CONSTANS (CO), which acts upstream of a graft-transmissible signal produced in leaves (*1*–*3*). Experiments with a dexamethasone-dependent, constitutively expressed version of CO have suggested that CO directly activates genes with diverse biochemical functions (*4*). These include two genes that are known to promote flowering: the transcription factor gene *SUPPRESSOR OF OVEREXPRESSION OF CONSTANS 1* (*SOC1*) and *FLOWERING LOCUS T* (*FT*), which encodes a small globular protein related to the floral repressor TERMINAL FLOWER 1 (TFL1) (*5*–*7*). In addition, *ACS10* and *P5CS2*, structural genes for ethylene and proline biosynthetic enzymes, were identified as potential CO targets in these experiments (*4*).

***FT* is the major primary target of CO in leaves.** Because the results with *CO* gain-of-function alleles had suggested that the CO-induced signal is complex, we used microarray analyses to identify targets of endogenous CO in leaves. To induce endogenous CO activity, we activated CO protein with light (*1*). We grew all plants in 8-hour short days. On the day of the experiment, we exposed the experimental group to 16 hours of light and the control group to 8 hours of light followed by 8 hours of darkness. We harvested leaves at the end of the 16-hour period. Differentially expressed genes were identified with a combination of per-gene variance [logit t test, $P < 0.025$ (*8*)] and common variance (>1.5× change).

Of 2000 genes that are activated or repressed after exposure to a single long day, merely three genes are responsive to long days in wild-type plants and at the same time differentially expressed between wild-type plants and *co* mutants in long days. Of these, only one gene does not respond at all to long days in a *co* background: *FT* (Fig. 1, A and B). In contrast, *SOC1*, *ACS10*, and *P5CS2* expression is independent of CO after exposure to a single long day (Fig. 1B), suggesting either that these genes respond only to higher levels of *CO* or that they respond to *CO* in tissues other than the leaf. In plants grown in continuous light, *FT* expression is much higher in leaves than at the shoot apex (Fig. 1C), consistent with leaves being the primary site of *FT* activation.

The finding that *FT* is the major target of *CO* in leaves is in agreement with our observation, also based on global expression profiles, that *FT* is the major output of *CO* at the shoot apex and that early floral markers such as *SOC1* and *FRUITFULL* (*FUL*) are similarly dependent on both *CO* and *FT* (*9*). Thus, the initial signal acting downstream of *CO* in leaves might be less complex than previously thought.

The bZIP protein FD is required for FT activity. To understand how FT activity is transduced, we searched for FT interactors. In a yeast two-hybrid screen, we isolated two closely related bZIP transcription factors, At2g17770 and At4g35900 (fig. S1), the *Arabidopsis* orthologs of tomato SIP8/SPGB, which interacts with *Arabidopsis* FT and TFL1, as well as the tomato TFL1 homolog SELF-PRUNING (*10*). The available collections of transferred DNA (T-DNA) insertion lines do not contain any At2g17770 alleles, but there are four different alleles but of At4g35900 (*11*). The late-flowering phenotype of these lines (Fig. 2A and Table 1) is rescued by a minigene, indicating that At4g35900 promotes flowering (fig. S2). The only late-flowering mutant described for this region of the genome is *fd*-1 (*12*), and complementation crosses showed *FD* and At4g35900 to be allelic. We therefore designated our reference insertion allele of At4g35900 as *fd*-2. By their phenotype and genetic interactions, *FD* and *FT* have been placed

[1]Department of Molecular Biology, [2]Arbeitsgruppe Lohmann, [3]Arbeitsgruppe Schmid, Max Planck Institute for Developmental Biology, 72076 Tübingen, Germany. [4]Salk Institute for Biological Studies, Plant Biology Laboratory, La Jolla, CA 92037, USA.

*These authors contributed equally to this work.
†Present address: John Innes Centre, Cell and Developmental Biology Department, Norwich NR4 7UH, UK.
‡To whom correspondence should be addressed. E-mail: philip.wigge@bbsrc.ac.uk (P.W.); weigel@weigelworld.org (D.W.)

FD, a bZIP Protein Mediating Signals from the Floral Pathway Integrator FT at the Shoot Apex

Mitsutomo Abe *et al.*

Science **309**, 1052 (2005);
DOI: 10.1126/science.1115983